Chen, Q., Zhai, Z., and Wang, L. 2007. Chemical Engineering Science, 62, 3580-3588.

Computer Modeling of Multiscale Fluid Flow and Heat and Mass Transfer in Engineered Spaces

Qingyan (Yan) Chen[a,*], Zhiqiang (John) Zhai[b], Liangzhu (Leon) Wang[a]

[a]*School of Mechanical Engineering, Purdue University, 585 Purdue Mall, West Lafayette, Indiana 47907-2088, USA*
[b]*Department of Civil, Environmental, and Architectural Engineering, University of Colorado at Boulder, UCB 428, ECOT 441, Boulder, CO 80309-0428, USA*

Abstract

Design and analysis of fluid flow and heat and mass transfer in engineered spaces require information of spatial scales ranging from 10^{-7} m to 10^{3} m and time scales from 10^{-1} s to 10^{8} s. The studies of such a multiscale problem often use multiple computer models, while each of computer models is applied to a small range of spatial and time scales. Accurate solution normally requires exchanging information between a macroscopic model and a microscopic model that can be done by coupling the two models. With the approach, it is possible to obtain an informative solution with the current computer memory and speed.

This paper used a few examples of fluid flow and heat and mass transfer in engineered spaces to conclude that a coupled macroscopic and microscopic model is likely to have a solution and the solution is unique. A stable solution for the coupled model can be obtained if some criteria are met. The information transfer between the macroscopic and microscopic models is mostly two ways. A one-way assumption can be accepted when the impact from small scale on large scale is not very significant.

Keywords: Multiscales; Computer modeling; Macroscopic; Microscopic

1. Introduction

"Engineered spaces" are any enclosed environments that are created to provide appropriate conditions and functionality for human and animal habitation. The conditions include thermal comfort, air quality, visual comfort, and acoustic comfort, etc. Examples of engineered spaces are commercial, institutional, and residential buildings; healthcare facilities; sport facilities; manufacturing plants; animal facilities; transportation vehicles (planes, trains, ships, and automobiles); and enclosed spaces for extreme environments (submarines and extraterrestrial vehicles). Although these enclosed spaces differ profoundly in terms of their shapes, functions, and surrounding environments, they are naturally or artificially maintained with appropriate conditions for habitation. The conditions in engineered spaces are always related to the surrounding environments, such as atmospheric environment, ocean, and universal space. The creation and maintenance of appropriate conditions in engineered spaces share many of the same technologies. For example, a computational fluid dynamics (CFD) program can be used to study

[*] Corresponding author: Tel.: +1 765 496 7562; fax: +1 765 496 7534.
E-mail address: yanchen@purdue.edu (Q. Chen).

airflow in different engineered spaces for study and design of air temperature, relative humidity, air velocity, and air quality. However, the spatial scales vary from 10^{-7} m to 10^3 m and time scales from 10^{-1} s to 10^8 s.

If an office building is used as an example, the study of air quality would require understanding movement of particulate matters from 0.1 microns (10^{-7} m) to 100 microns (10^{-4} m). The study of thermal comfort needs to know airflow and heat transfer in wall boundary layer from 1 mm (10^{-3} m) to 10 cm (10^{-2} m) thick and a spatial resolution from 10 cm (10^{-2} m) in a room and to 100 m (10^2 m) for a whole building. Since outdoor environment can have a significant influence on the interior environment of the building, the inclusion of building proximity of several street blocks into the study will bring the scale to a kilometer (10^3 m). By looking at the time scales, the study of thermal comfort would need turbulence intensity of airflow that is as small as a few Hz (10^{-1} s). The cycle of human breathing is in a scale of a second or two (10^0 s). The time constant from airflow in the office can be in the order of 10^1 s from a fan to 10^3 s without mechanical ventilation. Depending on the thermal mass in the building, the time constant for heat transfer through building structure is around 10^3 to 10^4 s. Thermal comfort study will need to understand the impact of outdoor climate that has a time scale of a day (10^5 s) to a year (10^8 s).

For such a complicated multiscale problem, solving all the information needed for all the scales with a detailed microscopic model may not be efficient (E and Engquist 2003). For example, CFD simulation of microscopic behavior, such as particle dispersion in a room, is too inefficient to be used in full detail for an entire building. On the other hand, we may be only interested in the macroscopic behavior of the engineered space, such as air quality between two zones in the building. Although the microscopic behavior and macroscopic behavior are linked, CFD is invalid in some parts of the computational domain (such as airflow through cracks between the two zones). Even if CFD can be used, it would require a computer with a huge memory and several months of computing time if CFD simulation is applied to the full spectrum of the spatial and time scales. Basic strategy is to use the detailed microscopic model as a supplement to provide the necessary information for extracting the macroscale behavior of the engineered space through a different model. If this is done properly, the combined macro-micro modeling technique will be much more efficient than solving entire system with the detailed microscopic model (E and Engquist 2003). This approach has become an essential part of computational science and engineering.

Thus, a multiscale problem in engineered spaces needs multiple computer models. Each of computer models is applied to a small range of spatial and time scales. With the approach, it is possible to obtain information needed with the current computer memory and speed. The information for the whole spectrum of the spatial and time scales is obtained by transferring critical information between two computer models that links two consecutive scales.

There are a few significant questions on such an approach. For example, do they still have a solution when they are coupled? If a solution exists, is it unique? Will the coupling lead to a stable and converged solution? Will the information transfer between the two computer models one way or two ways? This paper tries to answer these questions through a few examples.

2. Basic equations

Before we start to answer the questions, this section gives a brief description of two microscale CFD models and two macroscale models - an energy simulation model and a multizone airflow network model. All of the models are widely used in practice for analyzing and designing engineered spaces.

2.1 Governing equations for CFD

A CFD model solves a set of conservation equations that govern flow and heat and mass transfer in engineered spaces. The model has become an indispensable tool for gathering information to be used for design, control and optimization of engineered spaces. CFD can be divided into Direct Numerical Simulation (DNS), Large Eddy Simulation (LES), and the Reynolds Averaged Navier-Stokes equations with turbulence models (RANS modeling). DNS, which simulates all the scales of flow eddies, would require a fast computer that does not currently exist, and would take years of computing time for applications in an engineered space. Only LES and RANS modeling are appropriate with current computer power and memory so that they are used as microscale CFD models in this investigation.

RANS modeling separates all spatial parameters, such as velocity and temperature, into their mean and fluctuating components and the fluctuating components are only predicted with time-averaged root-mean-square (rms) values. Thus, RANS modeling solves only the mean components. For time-averaged and incompressible buoyant flow, the basic RANS equations are the continuity equation:

$$\frac{\partial(r U_i)}{\partial x_i} = 0 \qquad (1)$$

and the momentum equations:

$$\frac{\partial\left(\rho U_i\right)}{\partial t} + \frac{\partial\left(\rho U_j U_i\right)}{\partial x_j} = -\frac{\partial P}{\partial x_i} + \mu \frac{\partial^2 U_i}{\partial x_j \partial x_j} + \frac{\partial}{\partial x_j}\left(\rho \tau_{ij,t}\right),$$

(2)

where $\tau_{ij,t}$ are the eddy (turbulent) stresses that are modeled through a turbulent viscosity, μ_t:

$$\tau_{ij,t} = \frac{\mu_t}{\rho}\frac{\partial U_i}{\partial x_j}. \qquad (3)$$

If heat and mass transfer are involved, RANS equation for energy is

$$\frac{\partial}{\partial t}\left(\rho T\right) + \frac{\partial}{\partial x_j}\left(\rho U_j T\right) = \left(\frac{\mu}{\sigma_T} + \frac{\mu_t}{\sigma_{T,t}}\right)\frac{\partial}{\partial x_j}\left(\frac{\partial T}{\partial x_j}\right) \qquad (4)$$

and for species concentration is

$$\frac{\partial}{\partial t}\left(\rho C\right) + \frac{\partial}{\partial x_j}\left(\rho U_j C\right) = \left(\frac{\mu}{\sigma_C} + \frac{\mu_t}{\sigma_{C,t}}\right)\frac{\partial}{\partial x_j}\left(\frac{\partial C}{\partial x_j}\right). \qquad (5)$$

The turbulent viscosity μ_t in Equation (2)–(5) can be obtained with various turbulence models, such as the standard k-e model (Lauder and Spalding 1974).

LES is also based on Navier-Stokes equations. LES assumes that flow motion can be separated by large and small scale eddies through a filter. The large scale eddies are directly solved in LES, while the smaller scales are modeled. Since larger scale eddies carry the majority of the energy, they are more important. The smaller scales have been found to be more universal, and hence are more easily modeled. By filtering, one would obtain the continuity equation for the large-eddy motions as

$$\frac{\partial \rho \overline{u_i}}{\partial x_i} = 0 \tag{6}$$

and the momentum equations as

$$\frac{\partial \rho \overline{u_i}}{\partial t} + \frac{\partial}{\partial x_j}(\rho \overline{u_i} \cdot \overline{u_j}) = -\frac{\partial \overline{p}}{\partial x_i} + \mu \frac{\partial^2 \overline{u_i}}{\partial x_i \partial x_j} + \frac{\partial \rho \tau_{ij}}{\partial x_j} \ . \tag{7}$$

The bar represents grid filtering. For example, a one-dimensional filtered velocity can be obtained from

$$\overline{u_i} = \int G(x,x')\, u_i(x)\, dx' \tag{8}$$

where G(x, x'), the filter kernel, is a localized function. The G(x, x') is large only when (x-x′) is less than a length scale or a filter width. The length scale is a length over which averaging is performed. Flow eddies larger than the length scale are "large eddies" and smaller than the length scale are "small eddies".

The subgrid-scale Reynolds stresses in Eq. (7),

$$\tau_{ij} = \overline{u_i u_j} - \bar{u}_i \cdot \bar{u}_j \tag{9}$$

are unknown and are modeled by a subgrid-scale model. If necessary, one could easily obtain energy and species concentration equations for heat and mass transfer with a similar format like Eqs. (4) and (5) but with filtered variables.

The two CFD models, RANS modeling and LES, are often used to study flow and heat and mass transfer in engineered spaces with small spatial and time scales. This is because the CFD models can provide very detailed information but it would require significant computing effort. For larger spatial and time scale problems in engineered spaces, such as energy simulation over a year or flow and contaminant transport in a whole building, macroscopic models are used.

2.2 Governing equations for energy simulation

Energy simulation (ES) for an engineered space, especially for a building, is to determine heat gain and loss between the building and the environment. ES is normally performed with one-hour time step over one year of period. The maximum heat gain and loss are used for sizing the environmental control equipment. The hourly data is used to estimate the energy cost for operating the building, to determine thermal comfort level, and to identify the best control strategies for energy conservation. By assuming a uniform distribution of air temperature in each engineered space, ES solves two basic equations; one is heat conduction equation through the envelope of an engineered space

$$\frac{\partial T}{\partial t} = \frac{\partial}{\partial x_j}\left(\alpha \frac{\partial T}{\partial x_j} \right) \tag{10}$$

and the other is energy balance equation for the air in the engineered space

$$Q_{ecs} = \sum_{i=1}^{N} Q_i + Q_{int} - \frac{d\left(mC_pT\right)}{dt}. \tag{11}$$

Equations (10) and (11) can be obtained by simplifying the integral form of Eq. (4).

2.3 Governing equations for multizone airflow modeling

To predict the flow and contaminant transport in a large-scale engineered space such as a whole building, an appropriate macroscopic model is multizone airflow network model. The model represents each zone as an inter-connected node within a building airflow network. The program treats zone air temperature, pressure, and species concentrations as uniform whereas the localized effects within a given zone are overlooked. Empirical nonlinear mathematical models are utilized to represent airflow between zones. A multizone model often uses a power-law model to correlate the flow and the pressure difference across a crack or an opening between two engineered spaces as

$$F = C(\Delta P)^n. \tag{12}$$

Then the model solves air mass and species conservation equations for each engineered space as

$$\frac{dm}{dt} = \Sigma F \tag{13}$$

and

$$\frac{d\left(mC\right)}{dt} = \Sigma\left(FC\right) \tag{14}$$

Equation (12) is approximated from the integral form of Eq. (2). Equations (13) and (14) are integral form of Eqs. (1) and (5), respectively.

3. Solution existence and uniqueness

A macroscopic model, such as ES, assumes that temperature is uniform in each engineered space. Such an approximation allows the model to consider daily and seasonal temperature swings so the simulation can be conducted for a whole year cycle with a time step of one hour. If the details of the temperature distribution in an engineered space are needed, a microscopic model, such as CFD, is used. The CFD divides an engineered space into hundreds of thousands to millions of cells and the simulation will be with a time step of a few seconds. The two simulations deal with very different spatial scales (a building versus a room) and time scale (one hour versus a few seconds).

Theoretically, the two models can be coupled in order to obtain the information required via heat flux and temperature, if it is too costly to use the CFD model for energy simulation. Even though, the coupling can only be done in several days in a year as shown in Fig. 1 and the coupling in each day is done for a few times due to the large difference in time scale.

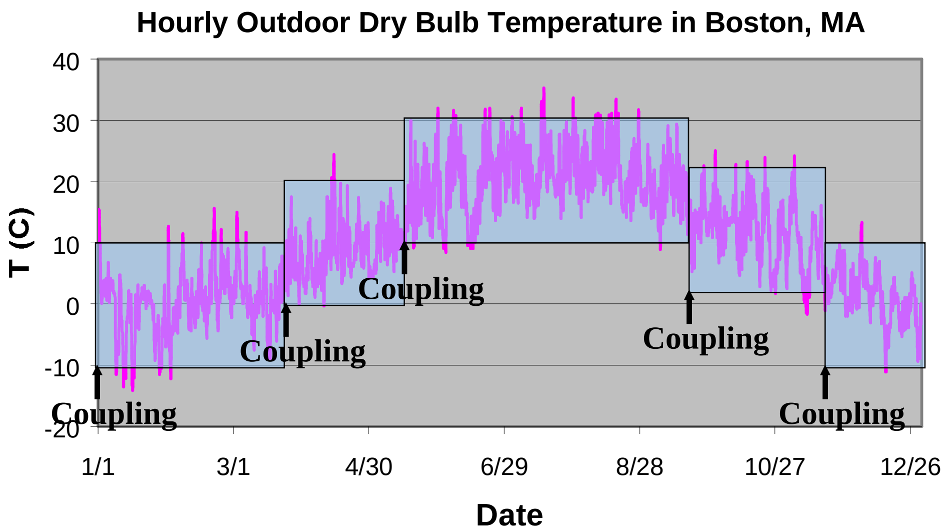

Fig. 1. Coupling of CFD with ES in a few days over a year.

Zhai and Chen (2003) considered the heat transfer on one interior surface of an engineered space in terms of conduction, convection, and radiation, and ignored the radiative heat flux from internal heat sources and solar radiation. They gave the following equation for heat transfer on one interior surface that interacts with other surfaces k for ES by assuming a homogenous wall

$$\sum_k h_{k,r}(T-T_k)+h_c(T-T_a)=\frac{K}{L}(T_o-T)\,. \tag{15}$$

With the equation, one can easily obtain

$$\frac{\partial T_a}{\partial T}=\frac{\sum h_{k,r}+h_c+\dfrac{K}{L}}{h_c}\in(1,\infty)\,. \tag{16}$$

If all the coefficients are assumed to be constant, then

$$\frac{\partial q_c}{\partial T} = \frac{\partial [h_c(T - T_a)]}{\partial T} = \frac{\partial h_c}{\partial T}(T - T_a) + h_c\frac{\partial (T - T_a)}{\partial T} = h_c(1 - \frac{\partial T_a}{\partial T}) < 0\,, \tag{17}$$

On the other hand, CFD focuses on the energy balance of indoor air, with the interior surfaces as the boundaries of the space. For cooling situation, the increase of the interior surface temperature T will increase the convective heat gain q_c (positive) and the air temperature T_a close to the wall. For the heating situation, the decrease of T will increase the convective heat loss q_c (negative) and decrease the air temperature T_a close to the wall. This means, $\frac{\partial q_c}{\partial T} > 0$ and $\frac{\partial T_a}{\partial T} > 0$. Therefore, with a constant h_c,

$$\frac{\partial q_c}{\partial T} = \frac{\partial [h_c(T - T_a)]}{\partial T} = \frac{\partial h_c}{\partial T}(T - T_a) + h_c\frac{\partial (T - T_a)}{\partial T} = h_c(1 - \frac{\partial T_a}{\partial T}) > 0\,. \tag{18}$$

The two equations will have an intersection (coupled solution) as shown in Fig. 2 although the curves are not necessarily straight because of the non-linearity of the complex problem. Thus, the coupled ES and CFD simulation has a solution.

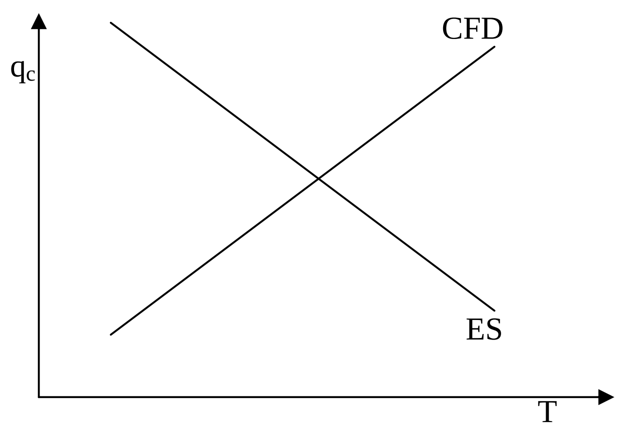

Fig. 2. Solution existence of coupled ES and CFD simulation.

The next question is whether there are multiple intersections (solutions) for the ES and CFD coupling. If there were multiple intersections, Fig. 3 illustrates two possible scenarios. Since the T_a-T slope for CFD is between 0 and 1 while that for ES is larger than 1, the scenario shown in Fig. 3(a) is impossible because the slope around point 2 does not satisfy the slope requirement. The scenario shown in Fig. 3(b) is also impossible because one specific surface temperature T in CFD can have only one corresponding T_a for a given situation (including given numerical models and techniques), and the same applies to ES. Therefore, there is one and only one solution for ES and CFD coupling.

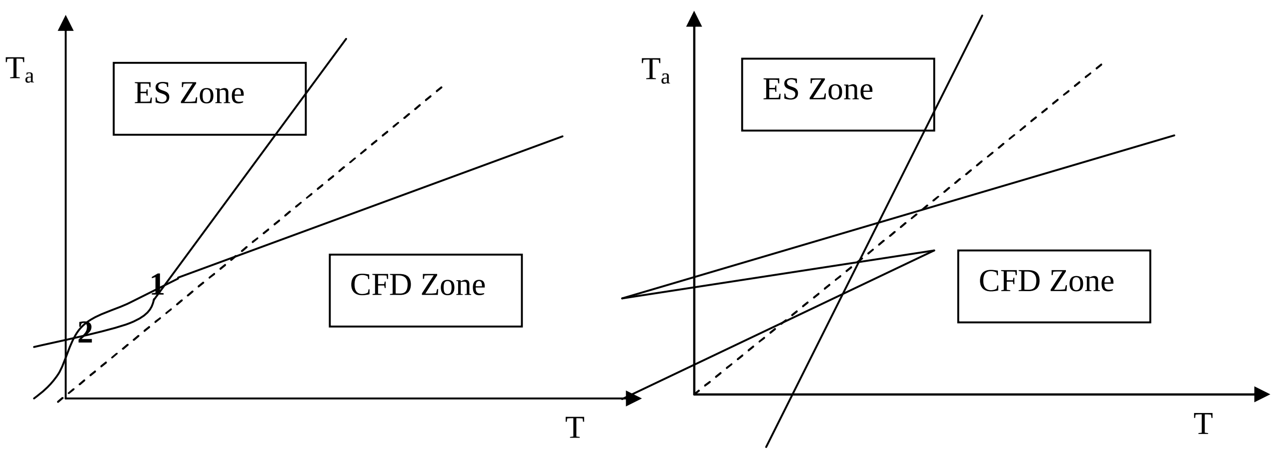

(a) (b)

Fig. 3 Assumed multiple intersections between T_a-T curves of ES and CFD.

The above example shows that the coupling between ES and CFD is done via q_c and T and T is the main parameter. Similarly, Wang and Chen (2005) used the same method to prove that a coupled multizone and CFD program has a solution and the solution is unique. The multizone model is a macroscopic model that assumes uniform distribution of air pressure and temperature and neglects air kinetic energy in a zone in an engineered space, such as a room in a building. The model calculates airflow and contaminant transport between zones using Eq. (12) through (14). In the coupled multizone (macroscopic model) and CFD (microscopic model) program, the coupling is done via flow rate and pressure. They used similar method as that used by Zhai and Chen (2003) where temperature was replaced by pressure and heat flux by flow rate.

In both cases, the macroscopic and microscopic models have demonstrated to have a solution and the solution is unique. Note that the equations solved by the macroscopic and microscopic models are from the same origin. The coupling procedure is a transfer of boundary conditions, such as temperature and heat flux as well as pressure and flow rate. Such a transfer should not have an impact on the solution. If such a philosophy could be extended to other coupled macroscopic and microscopic models with the same origin, it is likely that the conclusion of solution existence and uniqueness could be extended as well.

4. Solution stability and convergence

The unique solution of macroscopic and microscopic model coupling as shown in Section 3 may be obtained by different coupling methods. For ES and CFD coupling, Zhai and Chen (2003) showed four possible coupling methods. Different methods will lead to different assembled matrix equations that couple the macroscopic and microscopic models and exchange information between the two models. Not all of them are stable and can lead to a converged solution.

Similarly, Wang and Chen (2005) found three possible methods to couple a multizone model with CFD model for airflow simulation for a building:

1. multizone gives pressure to CFD and CFD returns pressure to multizone;

2. multizone gives pressure to CFD and CFD returns flow rate to multizone; and
3. multizone gives flow rate to CFD and CFD returns pressure to multizone.

The above coupling methods will result in different assembled matrix equations. When pressure and airflow rate boundary conditions are used together, such as in Methods 2 and 3, the assembled matrix equation is

$$\boldsymbol{CP} + \boldsymbol{F} = \boldsymbol{B}\,. \tag{19}$$

Howerver, when only pressure boundary conditions are employed (Method 1), the assembled matrix equation becomes

$$\boldsymbol{C_1P} = \boldsymbol{B_1}\,. \tag{20}$$

Different assembled matrix equations will not have the same numerical characteristics. The numerical performance of one matrix equation could be better than the others.

Scarborough (1966) established a convergent criterion for a Gauss-Seidel solution for a set of linear equations. The criterion is often used to evaluate CFD equations. In this study, multizone and CFD models provide complementary boundary conditions and the coupled model basically tries to obtain a Gauss-Seidel solution of the assembled matrix equation. Thus the Scarborough criterion could be used. For a Gauss-Seidel solution of the following linear equation system for Eqs. (19) and (20),

$$a_{f,P} f_P = \sum a_{f,nb} f_{nb} + b_f\,, \tag{21}$$

a sufficient convergence condition, the Scarborough criterion, is to satisfy the following ineqalities:

$$\frac{\sum |\, a_{f,nb} \,|}{|\, a_{f,P} \,|} \begin{cases} \le 1 \text{ for all equations} & \text{(22a)} \\ \\ < 1 \text{ for at least one equation.} & \text{(22b)} \end{cases}$$

The Scarborough criterion implies that the linear equation system for Eqs. (19) or (20), namely Eq. (21), will have a convergent solution if the matrix is ‘diagonally dominant’.

For Eq. (21), inequality (22b) can always be satisfied so long as at least one zone connects directly to another with a constant pressure in Eqs. (19) or (20). The multizone calculation itself actually requires that at least one zone with unknown pressure be connected to another with constant pressure. Otherwise, the airflow system in a multizone model will be singular and can have no unique solutions (Lorenzetti 2002). The zone with constant pressure can be the ambient pressure or a pressure specified. Inequality (22b) is therefore satisfied automatically in the coupled model.

Among the three methods, only Method 1 satisfies inequality (22a). In Eq. (20), each independent off-diagonal pressure will introduce its coefficient to that of the diagonal pressure of the matrix. Methods 2 and 3 solve Eq. (19) and ***F*** is an independent vector. The coefficients of ***F*** do not contribute to those of the diagonal pressure in the matrix. The condition of "diagonal dominance" may not always be satisfied for Eq. (19). Method 1 therefore is the only one that satisfies the Scarborough criterion and is guaranteed to have a convergent solution.

Since the Scarborough criterion is only a sufficient condition and the other two methods may still produce a convergent solution, it may be not convincing enough to conclude that Method 1 is the best method. A stability analysis should be performed to provide an in-depth investigation of the numerical performance of the coupling methods. Fig. 4 shows that, during a coupled solving procedure, the output of one model becomes the input of the other. When both inputs and outputs stabilize (their values do not change), the solution of the coupling is considered convergent. This iterative coupling procedure can be regarded as a closed-loop system. If r is the input parameter of a multizone model from CFD and r_k is its value at the coupling iteration k, we can define the difference of r at this iteration as $Dr_k = | r_{k+1} - r_k |$.

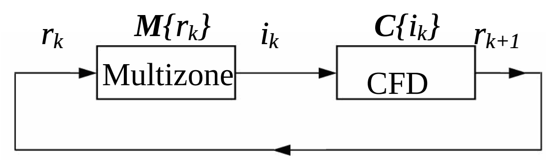

Fig. 4. Schematic of the coupling procedure at the coupling iteration k.

The system equation for a multizone model is $\boldsymbol{M}$, and its solution at iteration k, i_k, can be calculated as $i_k = \boldsymbol{M}\{ r_k \}$.Similarly, we have $r_{k+1} = \boldsymbol{C}\{ i_k \}$ for the CFD model. If Dr_k can be expressed by the partial derivatives of $\boldsymbol{M}$ and $\boldsymbol{C}$, we have

$$\Delta r_k = \left| \frac{\partial \boldsymbol{M}}{\partial r} \times \frac{\partial \boldsymbol{C}}{\partial i} \right| \times \Delta r_{k-1} = \left| \frac{\partial \boldsymbol{M}}{\partial r} \times \frac{\partial \boldsymbol{C}}{\partial i} \right|^k \times \Delta r_0 \ . \tag{23}$$

Then when k is sufficiently large, the coupled simulation will be stable and convergent only if

$$\left| \frac{\partial \boldsymbol{M}}{\partial r} \times \frac{\partial \boldsymbol{C}}{\partial i} \right| \leq 1. \tag{24}$$

Method 1 can satisfy Eq. (24) unconditionally so the method can always lead to a convergent and stable solution. Methods 2 and 3 may or may not satisfy Eq. (24) so they are conditionally stable.

Thus, the above results and those from Zhai and Chen (2003) conclude that different coupling methods for macroscopic and microscopic models may or may not yield a stable and converged solution, although the coupled model has a solution and the solution is unique.

5. Information transfer between macroscopic and microscopic models

The two sections above discussed the coupling of a macroscopic model (ES or multizone) with a microscopic model (CFD), because the understanding of the problem in macroscale requires information from microscale and vice versa. In many engineered spaces, one would be satisfactory with cascade information from macroscales and not necessary from microscales. For example, one would like to know how wind (macroscale) would have an impact on indoor thermal comfort and air quality (microscale). It may not be crucial to know how indoor temperature and contaminant concentration would change the atmospheric environment. Then the question is if one way transfer of the cascade information from macroscales to microscales would be acceptable in multiscale modeling of engineered spaces.

5.1 Example 1, Airflow within and around a building

If the building in Fig. 5 is used as an example, one-way transfer would normally assume that the building is a solid block so the airflow in building interior (microscale) would not have an impact on the airflow around the building (macroscale). For indoor thermal comfort and air quality analysis of the building, the airflow information around the solid block, such as the distributions of airflow, air velocity, pressure, air temperature, and contaminant concentrations, can be used as boundary conditions for further prediction of the distributions of the parameters in the building with actual building opening information. Such an approach could avoid the need to present very detailed information from microscale to macroscale, such as the impact of the openings of the building on airflow around the building. This will reduce the computing costs significantly since outdoor airflow (macroscale) calculation would need to deal with a flow domain of tens or hundreds of meters so it may not be practical to consider an opening of several centimeters from a room (microscale). If the airflow around the solid block building is similar to that around a building with open windows, then the cascade information from macroscales to microscales is acceptable.

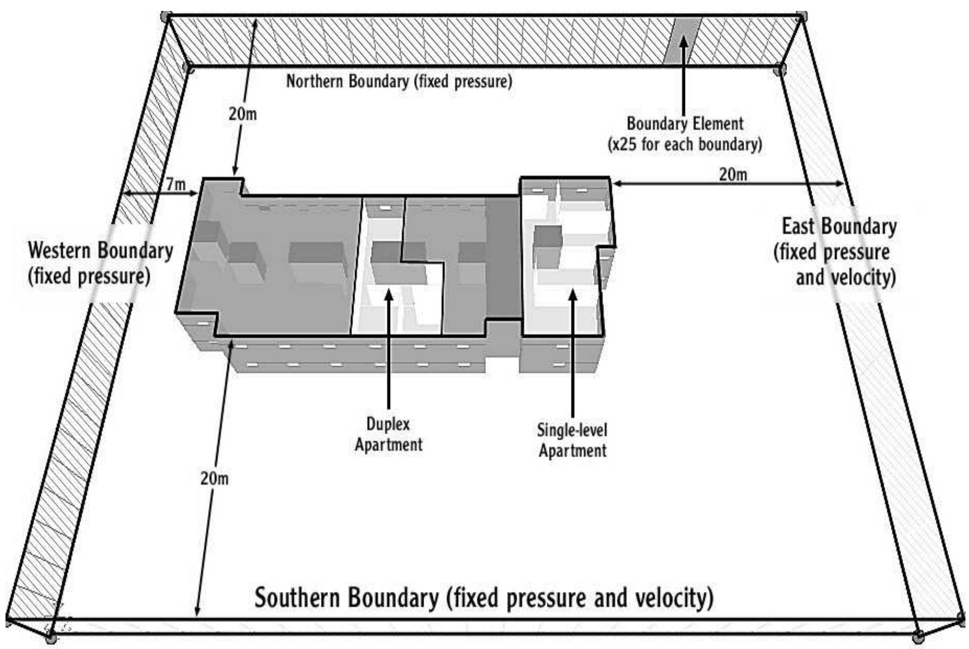

Fig. 5. Layout of a building and its proximity used as an example.

Fig. 6 shows the airflow around the building in a plane. Fig. 6(a) is the result using CFD only for the macroscale flow field (around the building with a solid block) and Fig. 6(b) for both macroscale and microscale (the building is with openings). Qualitatively, the two approaches compare very well for both pressure and airflow distributions. The flow patterns around the building correspond well with each other, with the main difference being the size of the main leeward vortex.

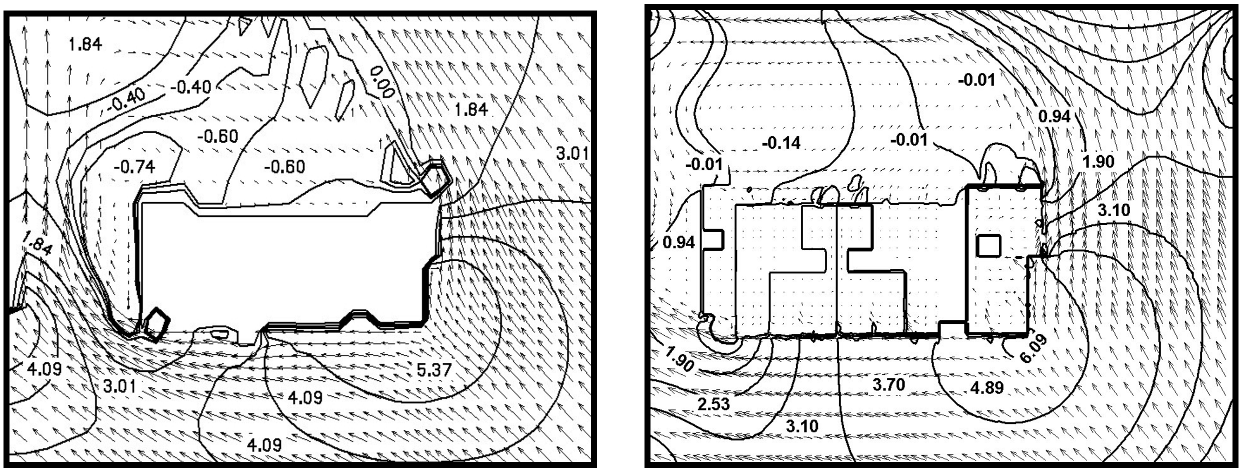

(a) (b)

Fig. 6. Simulation of airflow around the building with wind from south-east: (a) for one-way (macroscale only) and (b) for two-ways (both macroscale and microscale). The iso-lines and numerical values in the plots refer to static pressures in Pa.

There are some disparities in the two approaches when comparing pressure values. Fig. 6 shows the pressure distributions as well. Table 1 shows the average of the pressure values along all four faces of the building. The pressure and airflow data for the three models are taken at a plane halfway up the building that is centered vertically at a row of windows. It may be important to remember that the wind originates from the southeast. The pressure difference at the same building façade with the two approaches is between 0.41 to 1.81 Pa, compared with a pressure differential of 2.6 to 6.0 Pa between two opposite facades. This seems significant.

Table 1. Average relative pressures along each building face (Pa)

	North	South	East	West
One-way approach	-0.48	4.25	5.31	-0.79
Two-way approach	-0.09	3.84	3.70	1.02

Calculating the airflow rate through each apartment provides a more meaningful comparison of the indoor airflow results in terms of thermal comfort and air quality. With the pressure information on Table 1, Table 2 compares the airflow rate through two apartments in the building (see Fig. 5). The air change rate per hour (ACH) is the total airflow entering an apartment within one hour divided by the volume of the apartment. The air change rate was determined based on the pressure distribution around the building by using the orifice equation for the one-way approach. The results in Table 2 were obtained by using CFD only for the building. The differences in airflow rates are 5% for both the duplex and single-level apartments. It can therefore be concluded that these two approaches are similar. The total opening area used in Fig. 6(b) is 27% of the façade area. This is probably the upper limit that can be approximated as a solid block as in Fig. 6(a). There is no clear cut when to use the one-way approach and when to use the two-way approach. It is generally believed that the opening area should not exceed 20% of the façade area if the one-way approach is used. If opening area becomes larger, the impact of microscale model on macroscale model will be very evident.

Table 2. Comparison of air change rates per hour (ACH) for duplex and single-level apartments using the two approaches (ACH)

	One-way approach	Two-way approach
Single-level apartment	38	36
Duplex apartment	19	18

5.2 Example 2, Unsolved turbulence scale in LES

The one-way approach is not only used in resolved scale as discussed above but also in unsolved scale. For example, large eddy simulation has used subgrid scale model to transfer energy between resolved scale (macroscale) and unresolved scale (microscale) of motion. As pointed out by Bhushan et al. (2006), most models represent forward scatter (dissipation) of energy from resolved scale to unresolved scale but they fail to account for backscatter properly. Interesting enough, large eddy simulation with such subgrid scale models is widely used in engineered spaces and has yielded reasonably good results. Then, the question is if such backscatter of energy is significant.

This study used an LES model (Su et al. 2001) to obtain directly the unresolved quasi-Reynolds stresses by assuming a certain form of unfiltered quantities. The model is capable calculating backscatter. This investigation used the model to study turbulent flow around a circular cylinder with a sub-critical Reynolds number of 3900 that is often found in engineered spaces. The upstream and downstream boundaries are located at 10 and 20 times of the cylinder diameter, respectively, as shown in the left part of Fig. 7. The right part of Fig. 7 shows the grid distribution around the cylinder. Along the cylinder periphery, 120 grid points are evenly distributed. Jordan and Ragab (1998) found this circumferential resolution to be satisfactory for resolving Kolmogorov scale within the formation region at Re = 3400.

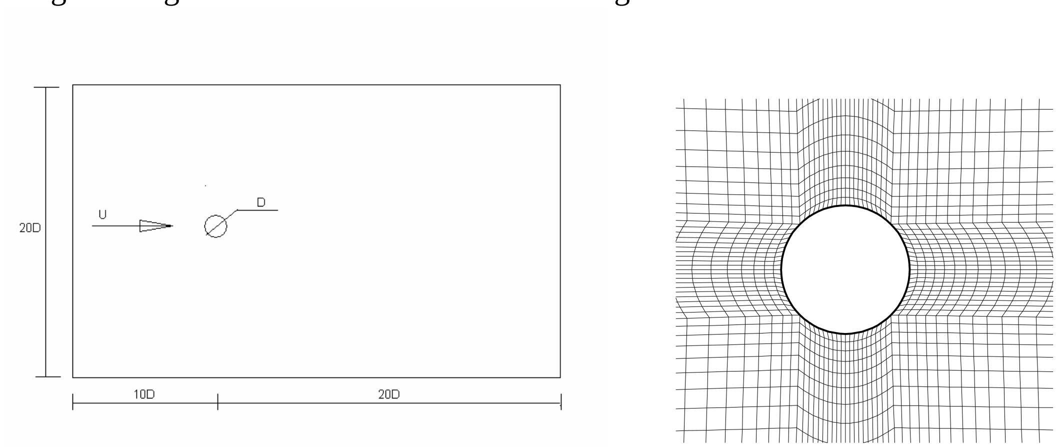

Fig. 7. The computational domain and the grid distribution around the cylinder.

Fig. 8 shows the averaged streamline results. The model can calculate the turbulence kinetic energy transfer from small vortices to large ones, also known as backscatter. In backscatter, the dissipation of the turbulence kinetic energy, $t_{ij}e_{ij}$. is negative. Fig. 9 shows the time-dependent dissipation of the turbulence kinetic energy at two different locations in a wake (the locations are marked in Fig. 8). The negative dissipation is dominant at the first location, while the positive dissipation is dominant at the second location. Therefore, the backscatter at the first location is more significant than that at the second location. Actually, the data analysis shows that the fluctuation of the turbulence energy dissipation in the near-wake region is much stronger than that in the far-wake region. Therefore, the backscatter often appears in the wake region near the cylinder, where the turbulent flow is more unstable than that in the regions far from cylinder. By studying the overall turbulence energy in the flow domain, the energy transfer from resolved scale to the unresolved scale is two to three times greater than the other direction. Therefore, other subgrid scale models can still achieve good results by considering only energy transfer from resolved scale to unresolved scale, although the backscatter can be dominant in some regions.

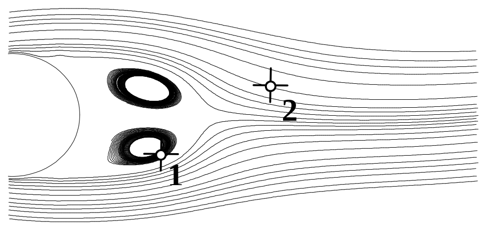

Fig. 8. Time averaged streamlines in the region.

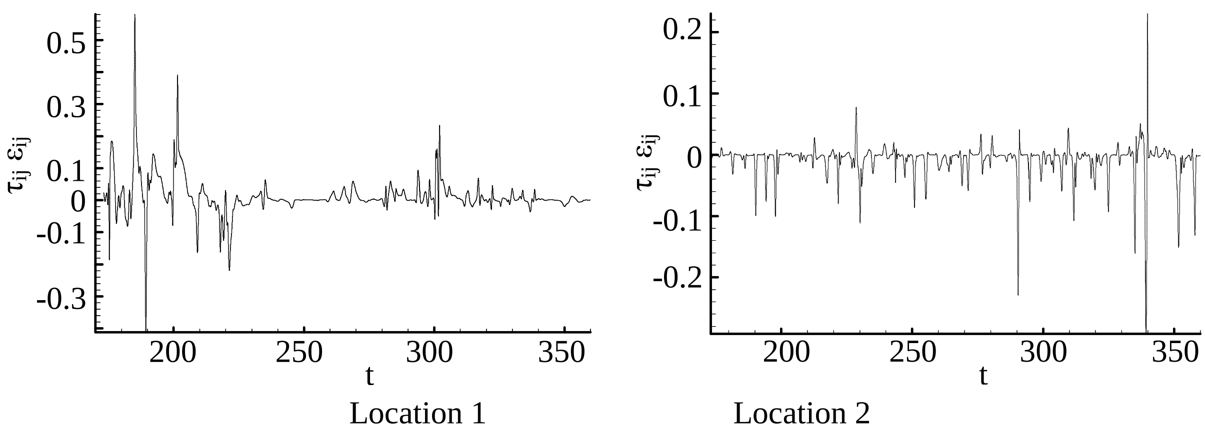

Fig. 9. Time-dependent negative energy dissipation at two locations in the wake.

The two examples in this section show that neglecting the impact of microscales on macroscales could be accepted if the contributions from the microscales are not very significant. In most engineered spaces, turbulence is very significant. One would not get correct flow distributions by conducting laminar flow simulations. The same conclusions can be applied for particle motions. It is acceptable to ignore the contributions of particle motion on main flow in an engineered space because the particle concentration is very low, but one cannot exclude the contributions of particle motion in a fluidized bed of a chemical reactor.

6. Conclusions

This paper uses engineered spaces as examples to demonstrate computer modeling of multiscale fluid flow and heat and mass transfer. Due to the large variation of spatial and time scales in engineered spaces, multiple computer models are needed to obtain necessary information. The following conclusions can be drawn from this study:

- When coupling a microscale model with a macroscale model based on the same origin of basic governing equations, the coupled model can have a solution for a problem and the solution is unique.
- The coupling requires information exchange between the two models. There are multiple methods for the information exchange. Not all the information exchange methods are stable and can lead to a converged solution. Certain criteria must be satisfied in order to obtain a stable and converged solution. The criterion for a converged solution of the coupling is that the coupled matrix equation is "diagonally dominant" (Equation 22). The criterion for a stable and convergent solution is when the product of the derivative of the governing equation to the input for each model is less than or equal to one (Equation 24).
- The impact of one model on the other is two-ways. However, the impact of macroscopic model on microscopic model is much more significant than the other way around. In many computer simulations of multiscale problems for engineered spaces, neglecting of the impact of microscale model on macroscale model is acceptable only when the contributions from the microscale are not very significant.

Notation

Latin alphabet

a	coefficient of an unknown variable
$\boldsymbol{B}$	vector of the source terms in the assembled total matrix equation
$\boldsymbol{B_1}$	vector of the source terms in the assembled total matrix equation for Method 1
$\boldsymbol{C}$	coefficient matrix in an assembled total matrix equation
C	mean species concentration
C	pressure coefficient for the opening
C_p	constant-pressure specific heat
$\boldsymbol{C_1}$	coefficient matrix in an assembled total matrix equation for Method 1
$\boldsymbol{F}$	the vector of unknown flow rates at the interface paths and cells
F	flow rate through an opening between two engineered spaces
G	filter kernel
h_c	interior convective heat transfer coefficient of the surface concerned
$h_{k,r}$	interior radiative heat transfer coefficient of the surface concerned
K	wall conductivity
L	wall thickness
$\boldsymbol{M}$	system equations for a multizone program
m	mass of air in an engineered space
n	exponent constant
$\boldsymbol{P}$	the unknown pressure vector of zones and cells
P	mean pressure
p	instantaneous pressure
Q_{ecs}	heat extracted by the environmental control system of an engineered space
Q_{ecs}	convective heat from internal equipment in an engineered space
q_c	convective heat flux from the surface concerned
r	input parameter for $\boldsymbol{M}$

T	air or surface temperature
T_a	indoor air temperature close to the surface concerned
t	time
U	mean velocity
u	instantaneous velocity
x	coordinate

Greek alphabet

a	thermal diffusivity
D	difference
ΔP	pressure drop through an opening between two engineered spaces
m	viscosity
r	density
s	Prandtle/Schmidt number
t	stresses
f	general variable

Subscripts/superscripts

a	air in an engineered space
i	index for coordinate or surface number
	index of the zones for a multizone program; input parameter for ***C***
j	index for coordinate
k	index of coupling iterations
	index for surface number
nb	neighboring
o	outside
P	index of grid points or cells
t	turbulence
f	general variable
-	*grid filtering*

Acknowledgements

The authors would like to thank C. Allocca, S.D. Hamilton, J. Huang, N. Kobayashi, and M. Su, for their contributions to the results published in this paper. This research is funded by Chinese Academy of Sciences, the U.S. National Science Foundation under grant CMS-9877118, the U.S. National Institute of Standards and Technology under agreement No. SB1341-04-Q-0771, and the U.S. Federal Aviation Administration (FAA) through the FAA Cooperative Agreement 04-C-ACE-PU for the Air Transport Center of Excellence for Airliner Cabin Environment Research (ACER). Although those organizations sponsored this project, they neither endorse nor reject the findings of this research.

References

Bhushan, S., Warsi, Z.U.A., Walters, D.K. 2006. Modeling of energy backscatter via an algebraic subgrid-stress model, AIAA Journal, 44(4), 837.

E, W., Engquist, B. 2003. Multiscale modeling and computation. Notices of the American Mathematical Society 50, 1062–1070.

Jordan, S.A., Ragab, S.A. 1998. A large eddy simulation of the near wake of a circular cylinder. Journal of Fluids Engineering, 120, 243-252.

Launder, B.E., Spalding, D.B. 1974. The numerical computation of turbulent flows. Computer Methods in Applied Mechanics and Engineering, Vol.3, pp. 269-289.

Lorenzetti, D.M. 2002. Computational aspects of nodal multizone airflow systems. Building and Environment, 37, 1083-1090.

Scarborough, J.B. 1966. Numerical mathematical analysis. Baltimore, The Johns Hopkins Press, MD, USA.

Su, M., Chen, Q., Chiang, C.-M. 2001. Comparison of different subgrid-scale models of large eddy simulation for indoor airflow modeling. Journal of Fluids Engineering, 123, 628-639.

Wang, L. and Chen, Q. 2005. On solution characteristics of coupling of multizone and CFD programs in building air distribution simulation. Proceedings of the 9th International IBPSA Conference (Building Simulation 2005), Montreal, Canada.

Zhai, Z., Chen, Q. 2003. Solution characters of iterative coupling between energy simulation and CFD programs. Energy and Buildings, 35(5), 493-505.